Photoinduced Electron Transfer between Acenaphthylene and Tetracyanoethylene: Effect of Irradiation Mode on Reactivity of the Charge-Transfer Complex and the Resulted Radical Ion Pair in Solution and Crystalline State

Naoki Haga,*[,†] Hiroyuki Nakajima,[†] Hiroaki Takayanagi,[†] and Katsumi Tokumaru[‡]

School of Pharmaceutical Sciences, Kitasato University, Minato-ku, Tokyo 108, Japan, and University of Tsukuba, Tsukuba, Ibaraki 305, Japan

Received February 3, 1998

The mechanism of photodimerization of acenaphthylene (ACN) and of reactions with tetracyanoethylene (TCNE) by electron transfer (ET) has been investigated in solution and solid state to elucidate the role of the radical cation of ACN ($ACN^{+\bullet}$) in formation of the *cisoid*-dimer (*cisoid*-**1**) and the *transoid*-dimer (*transoid*-**1**) of ACN and addition products to TCNE. Selective excitation of the 1:1 charge-transfer (CT) complex between ACN and TCNE with light of >500 nm did not result in any reaction in acetonitrile (AN) or 1,2-dichloroethane (DCE). On the other hand, direct irradiation of ACN with light of >400 nm in solution in the presence of TCNE gave *cisoid*-**1** and *transoid*-**1** as the major products together with a [2 + 2]-adduct (**2**) and two isomeric [2 + 2 + 2]-adducts (**3** and **4**) of ACN and TCNE as minor products. Distinction of photochemical reactivity between selective CT excitation and direct excitation of ACN can be attributed to faster backward electron transfer (BET) from the contact radical ion pair (CIP) on CT excitation than from the solvent-separated radical ion pair (SSIP) on direct excitation of ACN due to very low energy for BET, as low as 1.34 V. Effect of [TCNE] on quantum yield for the dimerization of ACN and on the *cisoid*/*transoid* ratio of the resulted **1** rationalizes the mechanism involving the singlet and triplet SSIP; the former tends to undergo BET, but the latter undergoes dissociation to $ACN^{+\bullet}$, followed by formation of dimeric radical cation of ACN, $ACN_2^{+\bullet}$, finally leading to **1**. A possible mechanism for formation of **3** and **4** is discussed on the basis of concentration dependence of ACN. Contrary to photochemical inertness of the CT complex in solutions, CT excitation of the 1:1 crystal of ACN and TCNE (ACN·TCNE) gave **2** as the sole product. The selective formation of **2** indicates that fixation of the two alkenic C=C double bonds in ACN·TCNE separated by 3−4 Å in both the excited CT state and the resulted CIP retards the deactivation and BET but enables them to undergo cycloaddition.

Introduction

Charge-transfer (CT) interaction between an electron donor and an acceptor in the ground state[1] and photoinduced electron transfer (ET)[2] have been accepted to be general phenomena in organic chemistry. The photochemical [2 + 2]-cycloaddition of alkenes in the presence of various electron acceptors has been studied as one of the representative models of cycloaddition of an alkene which proceeds via ET.[3−10] The mechanism which involves formation of a radical cation of alkenes followed by nucleophilic attack by another alkene molecule has been proposed for this reaction. However, due to the generally low yield of the cycloadducts and formation of undesirable polymeric products, it seems that until today less effort has been devoted to revealing the role of the singlet and triplet of alkene and the wavelength effect on reactivity and product distribution.

Acenaphthylene (ACN), one of the most simple nonalternant aromatic hydrocarbons, has been known to

† Kitasato University.

‡ University of Tsukuba.

(1) Foster, R. F. *Charge-Transfer Complexes in Organic Chemistry*; Academic Press: New York, 1963.

(2) (a) Mattes, R. F.; Farid, S. *Org. Photochem.* **1983**, *6*, 233−326. (b) Mattes, R. F.; Farid, S. *Acc. Chem. Res.* **1982**, *15*, 80−86. (c) Mattay, J. *Angew. Chem., Int. Ed. Engl.* **1987**, *26*, 825−845. (d) Mattay, J. *Synthesis* **1989**, 233−251. (e) Osa, T., Ed. *Kikan Kagaku Sosetsu*, No. 2; Gakkai Shuppan Center: Tokyo, 1988. (f) Oh-hashi, M., Ed. *Kagaku Sosetsu*, No. 33.; Gakkai Shuppan Center: Tokyo, 1982. (g) Kavarnos, G. J. *Fundamentals of Photoinduced Electron Transfer*; VCH Publishers: New York, 1993. (h) Leffler, J. E. *An Introduction to Free Radicals*; John Wiley & Sons: New York, 1993; pp 230−270.

(3) (a) Pages 75−96 in ref 2e. (b) Pages 38−54, 103−118 in ref 2g.

(4) Kricka, L. J.; Ledwith, A. *Synthesis* **1974**, 539−548.

(5) (a) Bell, F. A.; Crellin, R. A.; Fujii, H.; Ledwith, A. *J. Chem. Soc. Chem. Commun.* **1969**, 251−252. (b) Carruthers, R. A.; Crellin, R. A.; Ledwith, A. *J. Chem. Soc., Chem. Commun.* **1969**, 252−253.

(6) (a) Farid, S.; Shealer, S. E. *J. Chem. Soc., Chem. Commun.* **1973**, 677−678. (b) Mattes, S. L.; Farid, S. *J. Am. Chem. Soc.* **1982**, *104*, 1454−1456. (c) Farid, S.; Shealer, S. E. *J. Chem. Soc., Chem. Commun.* **1973**, 296−297. (d) Mizuno, K.; Kaji, R.; Otsuji, Y. *Chem. Lett.* **1977**, 1027−1030. (e) Pac, C.; Mizuno, K.; Sugioka, T.; Sakurai, H. *Chem. Lett.* **1973**, 187−188. (f) Calhoun, G. C.; Schuster, G. B. *J. Am. Chem. Soc.* **1986**, *108*, 8021−8027.

(7) (a) Asanuma, T.; Gotoh, T.; Tsuchida, A.; Yamamoto, M.; Nishijima, Y. *J. Chem. Soc., Chem. Commun.* **1977**, 485−486. (b) Yamamoto, M.; Asanuma, T.; Nishijima, Y. *J. Chem. Soc., Chem. Commun.* **1975**, 53−54. (c) Asanuma, T.; Yamamoto, M.; Nishijima, Y. *J. Chem. Soc., Chem. Commun.* **1975**, 56−57, 608−609. (d) Kojima, M.; Sakuragi, H.; Tokumaru, K. *Tetrahedron Lett.* **1981**, *22*, 2889−2892.

(8) (a) Mattes, S. L.; Farid, S. *J. Am. Chem. Soc.* **1986**, *108*, 7356−7361. (b) Mattes, S. L.; Farid, S. *J. Am. Chem. Soc.* **1983**, 105, 1386−1387. (c) Arnold, D. R.; Neunteufel, R. A. *J. Am. Chem. Soc.* **1973**, *95*, 4080−4081.

(9) Kuwata, S.; Shigemitsu, Y.; Odaira, Y. *J. Chem. Soc., Chem. Commun.* **1972**, 2.

(10) (a) Ohashi, M.; Tanaka, Y.; Yamada, S. *Tetrahedron Lett.* **1977**, *41*, 3629−3632. (b) Ohashi, M.; Tanaka, Y.; Yamada, S. *J. Chem. Soc., Chem. Commun.* **1976**, 800.

S0022-3263(98)00182-0 CCC: $15.00
Published on Web 07/08/1998

Scheme 1

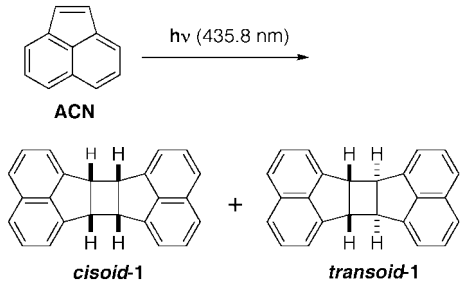

undergo dimerization on irradiation into two isomeric dimers (*cisoid*-**1** and *transoid*-**1**)[11−16] in quantitative yield (Scheme 1). The mechanism of this reaction has been extensively studied, because of different stereoselectivity for dimerization from the singlet and triplet states[13−16] together with unique photophysical properties such as short lifetime of its singlet (S_1) state,[17,18] very weak fluorescence,[18] and extremely low quantum yield for intersystem crossing, Φ_{ST}.[19,20] It has been concluded that on direct irradiation of ACN, *transoid*-**1** is formed from the triplet (T_1) state and *cisoid*-**1** is derived from both the S_1 and T_1 states, though mainly from the former.[13,14] Our recent study has clearly quantified the role of the pathways from the S_1 and T_1 states, based on quantum yields for the reaction in solutions over a wide range of concentrations of ACN and the effect of a triplet sensitizer, a triplet quencher, and heavy atom-containing solvents.[21]

On the other hand, photochemical reactions of ACN in the presence of electron acceptors have not been studied except by Shirota and co-workers.[22] Because on irradiation with 435.8 nm monochromatic light ACN is converted into the isomeric dimers without producing byproducts such as polymers,[14b,21] we considered that ACN is an appropriate model to study the photodimerization via ET, focusing on the effect of reduction potential of the acceptor and concentration of the donor and the acceptor on quantum yields and product distribution.

Photoinduced ET between electron donors and acceptors can be classified into two categories in terms of the mode of production of the radical ions, i.e., ET at encounter between an excited state and a ground state where no interaction occurs in their ground states and ET occurring on excitation of the ground-state CT complex.[23] Mataga and co-workers,[24,25] have observed that, in some donor−acceptor systems, radical ion pairs resulting from excitation of the CT complex undergo backward electron transfer (BET) with larger rate constants, k_{BET}, than those from the encounter mode in the same solvents. It follows that, if the CT complex could be irradiated independently, distinctive features in photochemical reactivity due to the difference of k_{BET} should be observed between the two modes of excitation.

Tetracyanoethylene (TCNE),[26] which is one of the most powerful electron acceptors with a reduction potential ($E_{1/2}^{Red}$) of 0.24 V (vs SCE in AN),[27] forms a brown-colored CT complex with ACN in the ground state. Because selective excitation of the CT band is readily accomplished, we have chosen the ACN−TCNE system as a suitable one to examine distinction between the two modes of irradiation.

Apart from reactivity on irradiation in solution, photochemical reactions in solid states have received much attention and have been developed due to its specific features such as stereoselectivity, regioselectivity (specificity), and generation of chirality.[28] Many CT complexes can be isolated as crystals whose crystal structures have been elucidated by X-ray crystallographic technique.[29] Though the physical properties of crystalline CT complexes have been investigated due to their intriguing properties such as ferromagnetism,[30] few studies have so far been done on their photochemical behavior in the crystal.[31] Irradiation of crystalline CT complexes must provide a unique opportunity to study the reactions via ET included in a highly organized crystalline lattice.

To elucidate the mechanisms of the photochemical reactions of ACN involving ET, we focused herein on three points as follows: (1) examine the wavelength effect of irradiation to compare reactivity of CIP and the SSIP, (2) determine product distribution and quantum yields on irradiation of ACN−TCNE system over a wide range of concentrations of ACN and TCNE to elucidate the participation of ET from the S_1 and T_1 states of ACN,

(11) (a) Dziewonski, K.; Rapalski, G. *Chem. Ber.* **1912**, *45*, 2491−2495. (b) Dziewonski, K.; Paschalski, C. *Chem. Ber.* **1913**, *46*, 1986−1992. (c) Dziewonski, K.; Leyko, Z. *Chem. Ber.* **1914**, *47*, 1679−1990.
(12) (a) Bowen, E. J.; Marsh, J. D. F. *J. Chem. Soc.* **1947**, 109−110. (b) Griffin, G. W.; Veber, D. F. *J. Am. Chem. Soc.* **1960**, *82*, 6417. (c) Hartmann, I.; Hartmann, W.; Schenck, G. O. *Chem. Ber.* **1967**, *100*, 3146−3155. (d) Devidson, R. S. *J. Chem. Soc., Chem. Commun.* **1969**, 1450−1451. (e) Plummer, B. F.; Hall, R. A. *J. Chem. Soc., Chem. Commun.* **1970**, 44−45.
(13) Livingston, R.; Wei, K. S. *J. Phys. Chem.* **1967**, *71*, 541−547.
(14) (a) Cowan, D. O.; Drisco, R. L. *Tetrahedron Lett.* **1967**, 1255−1258. (b) Cowan, D. O.; Drisco, R. L. *J. Am. Chem. Soc.* **1970**, *92*, 6286−6291. (c) Cowan, D. O.; Drisco, R. L. *J. Am. Chem. Soc.* **1970**, *92*, 6281−6285. (d) Cowan, D. O.; Kozier, J. C. *J. Am. Chem. Soc.* **1974**, *96*, 1229−1230. (e) Cowan, D. O.; Kozier, J. C. *J. Am. Chem. Soc.* **1975**, *97*, 249−254.
(15) Koser, G. F.; Liu, V.-S. *J. Org. Chem.* **1978**, *43*, 478−481.
(16) White, E. H.; Wildes, P. D.; Wiecko, J.; Doshan, H.; Wei, C. C. *J. Am. Chem. Soc.* **1973**, *95*, 7050−7058.
(17) Samanta, A.; Devadoss, C.; Fessenden, R. W. *J. Phys. Chem.* **1990**, *94*, 7106−7110.
(18) (a) Brown, E. J. *Advances in Photochemistry*; John Wiley and Sons: New York, 1963; Vol. 1, pp 23−42. (b) Plummer, B. F.; Hopkinson, M. J.; Zoeller, J. K. *J. Am. Chem. Soc.* **1979**, *101*, 6779−6781. (c) Castellan, G.; Dumartin, G.; Bouas-Laurent, H. *Tetrahedron* **1980**, *36*, 97−103.
(19) Dunsbach, R.; Schmidt, R. *J. Photochem. Photobiol. A: Chem.* **1994**, *83*, 7−13.
(20) Samanta, A.; Fessenden, R. W. *J. Phys. Chem.* **1989**, *93*, 5823−5827.
(21) Haga, N.; Takayanagi, H.; Tokumaru, K. *J. Org. Chem.* **1997**, *62*, 3734−3743.
(22) Shirota, Y.; Nagata, J.; Mikawa. *Chem. Lett.* **1972**, 49−50.
(23) **23.** Mataga, N. *Photochemical Energy Conversion*; Elsevier: Amsterdam, 1989; pp 32−46.
(24) (a) Miyasaka, H.; Ojima, S.; Mataga, N. *J. Phys. Chem.* **1989**, *93*, 3380−3382. (b) Ojima, S.; Miyasaka, H.; Mataga, N. *J. Phys. Chem.* **1990**, *94*, 5834−5839.
(25) (a) Asahi, T.; Ohkohchi, M.; Mataga, N. *J. Phys. Chem.* **1993**, *97*, 13132−13137. (b) Mataga, N.; Shioyama, H.; Kanda, Y. *J. Phys. Chem.* **1987**, *91*, 314−317. (c) Ojima, S.; Miyasaka, H.; Mataga, N. *J. Phys. Chem.* **1990**, *94*, 7534−7539. (d) Miyasaka, H.; Nagata, T.; Kiri, M.; Mataga, N. *J. Phys. Chem.* **1992**, *96*, 8060−8065. (e) Asahi, T.; Mataga, N. *J. Phys. Chem.* **1989**, *93*, 6575−6578. (f) Asahi, T.; Ohkohchi, M.; Matsusaka, R.; Mataga, N.; Zhang, R. P.; Osuka, A.; Maruyama, K. *J. Am. Chem. Soc.* **1993**, *115*, 5665−5674. (g) Asahi, T.; Mataga, N. *J. Phys. Chem.* **1991**, *95*, 1956−1963.
(26) (a) Fatiadi, A. J. *Synthesis* **1986**, 249−284; (b) **1987**, 749−789.
(27) (a) Mulvaney, J. E.; Cramer, R. J.; Hall, H. K. *J. Polym. Sci., Polym. Chem. Ed.* **1983**, *21*, 309−314. (b) Olbrich-Deussner, B.; Kaim, W.; Gross-Lannert, R. *Inorg. Chem.* **1989**, *28*, 3113−3120.
(28) Ramamurthy, V., Ed. *Photochemistry in Organized and Constrained Media*; VCH Publishers: New York, 1991.
(29) Pages 216−251, 276−302 in ref 1.
(30) Kollmac, C.; Kahn, O. *Acc. Chem. Res.* **1993**, *26*, 259−265.
(31) (a) Suzuki, T.; Fukushima, T.; Yamashita, Y.; Miyashi, T. *J. Am. Chem. Soc.* **1994**, *116*, 2793−2803. (b) Koshima, H.; Ding, K.; Chisaka, Y.; Matsuura, T.; Ohashi, Y.; Mukasa, M. *J. Org. Chem.* **1996**, *61*, 2352.

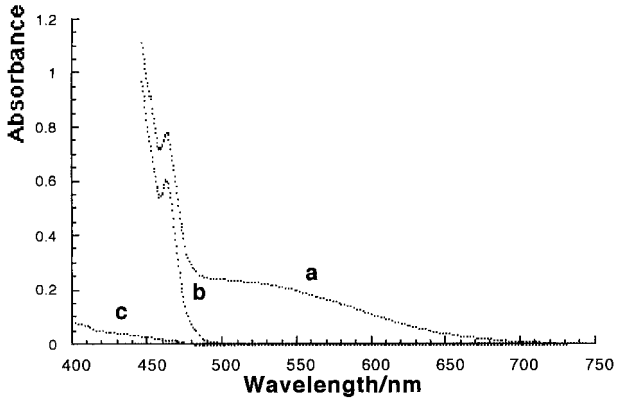

Figure 1. Absorption spectra in DCE: (a) CT complex of ACN and TCNE ([ACN] = 2.5×10^{-2} M and [TCNE] = 1.0×10^{-2} M); (b) ACN (2.5×10^{-2} M); (c) ACN (8.0×10^{-4} M). TCNE is transparent in this wavelength region.

Scheme 2

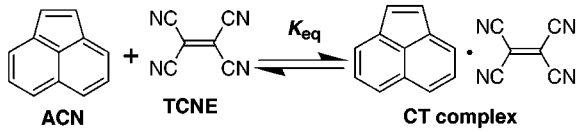

and (3) irradiate the crystalline CT complex of ACN and TCNE to examine characteristic features to the photoinduced ET in the organic solid state. Furthermore, as a reference, we also made irradiation of the ACN in the presence of fumaronitrile (FN), which is a weaker acceptor than TCNE and does not form a CT complex with ACN in the ground state.

Results

CT Complex. When a solution of TCNE was added to a solution of ACN in DCE or AN, immediately tan-brown coloration developed. Figure 1 shows the absorption spectra accompanying this spectral change together with that of ACN in DCE. Since neither ACN nor TCNE absorbs in the 460−700-nm visible region, the broad absorption band is readily assigned to a CT complex produced between ACN and TCNE (Scheme 2), as reported for CT complexes of various aromatic hydrocarbons with TCNE.[26,29,32−35] The CT band in Figure 1 is not well-separated from the absorption band of ACN in the region of 400−500 nm. Therefore, the λ_{max} of the CT complex seems concealed among the intensive absorption of ACN. However, according to the empirical equation relating the charge-transfer energies with ionization potential of donors,[36] the λ_{max} can be estimated as 480 nm, which agrees with the present outcome.

The equilibrium constant, K_{eq}, of the CT complex between ACN and TCNE was determined spectrophotometrically by the Benesi−Hildebrand procedure.[37] Thus the absorbance due to the CT band, A_{CT}, was determined at 520 nm to avoid overlap with the absorption of ACN with varying concentration of ACN and TCNE to get K_{eq} for the 1:1 CT complex (Scheme 2) by eq 1.

$$\frac{[\mathrm{TCNE}]}{A_{\mathrm{CT}}} = \frac{1}{\epsilon_{\mathrm{CT}}} + \frac{1}{\epsilon_{\mathrm{CT}} K_{\mathrm{eq}} [\mathrm{ACN}]} \qquad (1)$$

Here, ϵ_{CT} represents the molar extinction coefficient of the CT complex at 520 nm (instead of ϵ at maximum wavelength, λ_{max}). By employing eq 1, K_{eq} is determined as 1.54 ± 0.23 and 2.20 ± 0.38 M^{-1} with ϵ_{CT} of 1320 and 500 M^{-1} cm^{-1} in DCE and AN, respectively. Relatively small values for K_{eq} in both solvents are similar to those of other CT complexes of TCNE[38] and indicate that the intermolecular interaction between ACN and TCNE is moderate.

Irradiation of ACN in the Presence of TCNE in Solution. When a solution containing 1.0×10^{-2} M ACN and 1.0×10^{-2} M TCNE in AN or DCE was irradiated with >500-nm light to excite the CT band of the complex selectively, the color from the complex did not bleach at all after 24 h of exposure of the light. Thin-layer chromatography (TLC) or ^{1}H NMR analysis of the solution showed that no reaction occurred on the CT excitation.

However, on irradiation of this solution with light of wavelength longer than 400 nm, which excites uncomplexed ACN, ACN was converted into a [2 + 2]-cycloadduct (**2**) between ACN and TCNE and [2 + 2 + 2]-cycloadducts (**3** and **4**) together with *cisoid*-**1** and *transoid*-**1** as characterized by chromatographic isolation (Scheme 3).

The structure of **2**[22,36] was identified by comparison of the spectral properties with that of an authentic sample which was prepared by an alternative method. Compositions of **3** and **4** were deduced by mass spectroscopy and elemental analysis. The structure of **3** was established successfully by X-ray crystallography of a single crystal. The crystallographic data are given in Table 1. The ORTEP diagram in Figure 2 shows that this compound has a structure with the apparent stereoselective reaction of two molecules of ACN with one molecule of TCNE, where the four methine protons originating from alkenic ones of ACN are arranged asymmetrically. In the ^{1}H NMR spectrum, the pair of double-doublet resonance at δ 4.68 and 5.02 is readily assigned to H_2 and H_3, respectively. Similarly, the pair of doublet at δ 4.28 and 4.68 is assigned to H_1 and H_4, respectively, with coupling constants (J) of 10.8, 5.3, and 6.2 Hz for J_{1-2}, J_{2-3}, and J_{3-4}, respectively. Though the conformation of the cyclohexane ring of **3** is not a typical chair form, the J values of the protons in this ring are similar to those of axial−axial and axial−equatorial protons in a cyclohexane ring with a chair form. The configurations of the aliphatic tertiary protons in **4** were determined on the basis of comparison of its ^{1}H NMR spectrum with that of **3**. Thus, 12 nonequivalent aromatic protons and 4 nonequivalent aliphatic tertiary protons agree with asymmetric structure similar to that in **3**. Chemical shifts of H_1, H_2, H_3, and H_4 are 4.56, 4.36, 4.71, and 4.64, respectively, with J_{1-2}, J_{2-3}, and J_{3-4} of 10.5, 10.0, and 6.7 Hz, respectively.

(32) (a) Cram, D. J.; Bauer, R. H. *J. Am. Chem. Soc.* **1959**, *81*, 5971−5977. (b) Sheehan, M.; Cram, D. J. *J. Am. Chem. Soc.* **1969**, *91*, 3553−3558.

(33) Kuroda, H.; Ikemoto, I.; Akamatsu, H. *Bull. Chem. Soc. Jpn.* **1966**, *39*, 1842−1849.

(34) Vincent, V. M.; Wright, J. D. *J. Chem. Soc. Faraday 2* **1974**, *70*, 58−71.

(35) Eckhardt, C. J.; Hood, R. J. *J. Am. Chem. Soc.* **1979**, *101*, 6170−6174.

(36) Shirota, Y.; Nagata, J.; Nakano, Y.; Nogami, T.; Mikawa, H. *J. Chem. Soc., Perkin Trans. 2* **1977**, 14−18.

(37) (a) Pages 125−178 in ref 1. (b) Benesi, H. A.; Hildebrand, J. H. *J. Am. Chem. Soc.* **1949**, *71*, 2703−2707.

(38) Pages 276−302 in ref 1.

Scheme 3

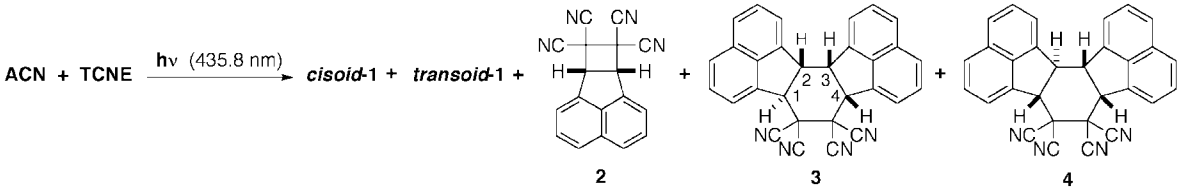

2 **3** **4**

Table 1. Crystal Data for 3, 7, and ACN·TCNE

	3	**7**	ACN·TCNE
empirical formula	$C_{30}H_{16}N_4$	$C_{16}H_{10}N_2$	$C_{18}H_8N_4$
color, habit	colorless, prism	colorless, prism	tan-brown, prism
dimensions (mm)	0.30 × 0.30 × 0.20	0.20 × 0.20 × 0.20	0.40 × 0.60 × 0.30
crystal system	orthorhombic	orthorhombic	monoclinic
lattice parameters	a = 21.258(3) Å	a = 9.841(2) Å	a = 7.240(1) Å
	b = 23.556(3) Å	b = 21.813(2) Å	b = 7.680(1) Å
	c = 9.451(2) Å	c = 5.405(1) Å	c = 26.548(9) Å
	V = 4733(1) Å^3	V = 1160.3(5) Å^3	V = 1468(5) Å^3
			β = 96.02(8)°
space group	*Pbca* (No. 61)	$P2_12_12_1$ (No. 19)	$P2_1/n$ (No. 14)
Z value	8	4	4
D_{calc} (g cm^{-3})	1.259 (1.223)[a]	1.318	1.268
no. reflections measured	4716	1244	2813
no. reflections for structure solution and refinement	1468	1034	1157
R	0.085	0.060	0.094
R_w	0.074	0.068	0.098

[a] Determined value in aqueous potassium iodide.

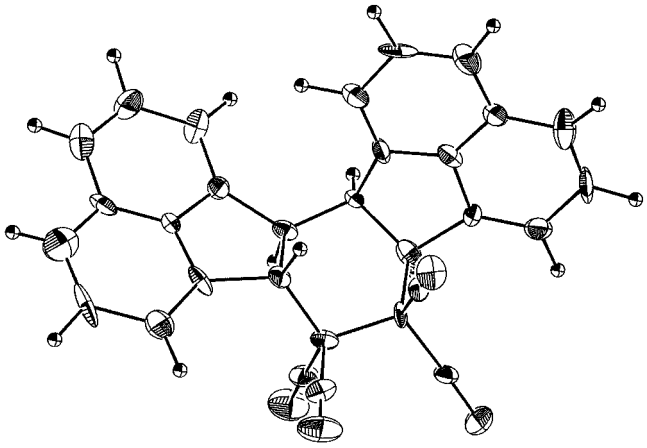

Figure 2. ORTEP drawing of compound **3**.

When each of the dimers (*cisoid*-**1** and *transoid*-**1**) and **2** was irradiated (λ > 400 nm) independently in the presence of TCNE, the starting compound was completely recovered without producing **3** and **4** at all. Furthermore, all of those five products (*cisoid*-**1**, *transoid*-**1**, **2**−**4**) were stable against irradiation of this wavelength of light without producing any photochemical secondary products.

Effects of concentration of ACN and TCNE on product distribution were examined on irradiation (λ > 400 nm) with the conversion of ACN in the range of 35−70%. The results are collected in Table 2. In each case, yields of *cisoid*-**1** and *transoid*-**1** are higher than those of **2**−**4** even under conditions with excess of TCNE. It is noteworthy that *cisoid*-**1** prevails over *transoid*-**1** in the presence of TCNE in each solvent. Among **2**−**4**, yields of **3** and **4** are higher than that of **2** at high concentrations of ACN (1.0×10^{-1} M) in the presence of TCNE ≥ 1.0×10^{-2} M, whereas the opposite was the case in irradiation at low concentration of ACN. No priority was observed between **3** and **4**.

Table 2. Product Distribution on Direct Irradiation of ACN with Light of Longer Wavelength than 400 nm in the Presence of TCNE in DCE and AN

			yield (%)[a]					
[ACN] (M)	[TCNE] (M)	solvent	*cisoid*-**1**	*transoid*-**1**	*cisoid*/*transoid*	**2**	**3**	**4**
10^{-3}	0	DCE	37	63	0.59			
10^{-3}	10^{-3}	DCE	78	16	4.75	6	0	0
10^{-3}	10^{-2}	DCE	80	15	5.33	5	0	0
10^{-3}	10^{-1}	DCE	80	15	5.33	5	0	0
10^{-1}	0	DCE	43	57	0.74			
10^{-1}	10^{-3}	DCE	48	47	1.02	5	0	0
10^{-1}	10^{-2}	DCE	67	19	3.29	3	5	5
10^{-1}	10^{-1}	DCE	74	11	6.80	2	7	6
10^{-3}	0	AN	63	37	1.67			
10^{-3}	10^{-3}	AN	82	15	5.60	3	0	0
10^{-3}	10^{-2}	AN	83	12	6.80	4	0	0
10^{-3}	10^{-1}	AN	81	12	6.75	6	0	0
10^{-1}	0	AN	68	32	2.15			
10^{-1}	10^{-3}	AN	77	18	4.25	5	0	0
10^{-1}	10^{-2}	AN	80	11	7.28	3	3	2
10^{-1}	10^{-1}	AN	78	8	9.20	3	5	5

[a] Yields based on consumed ACN determined by ^{1}H NMR with conversion of ACN of 35−60%.

Quantum Yields and *cisoid*-1/*transoid*-1 Ratio (*Cisoid/Transoid* Ratio) in the Photodimerization of ACN in the Presence of TCNE. To quantify the influence of concentration of TCNE on the efficiency and the stereoselectivity of the dimerization of ACN, quantum

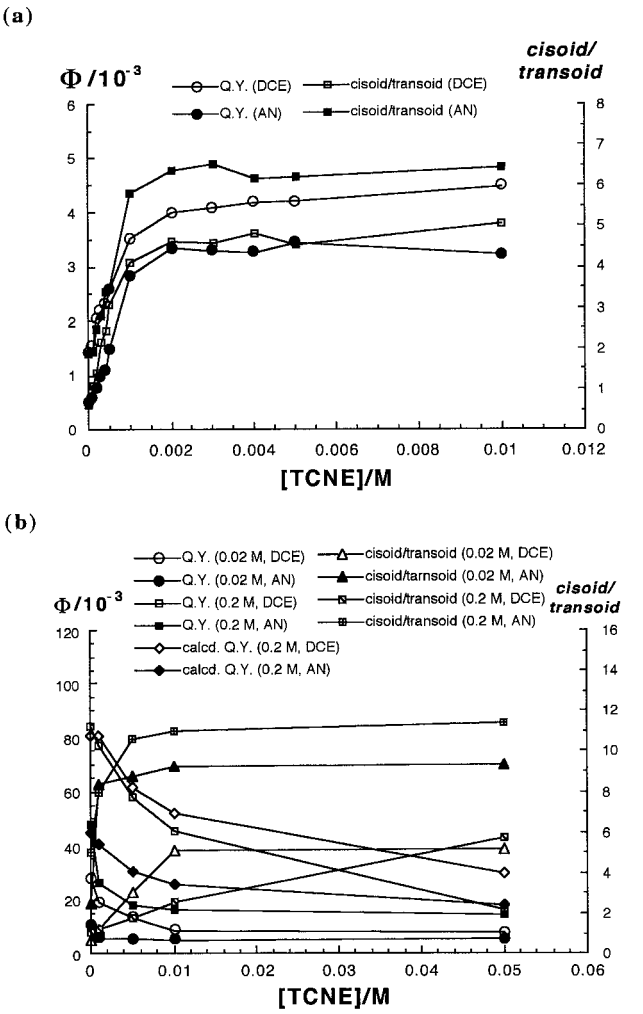

Figure 3. Plots of quantum yield (Q.Y.) for photodimerization of ACN, Φ_R, and the *cisoid/transoid* ratio versus concentration of TCNE, [TCNE], in DCE and AN: (a) [ACN] = 1.0×10^{-3} M; (b) [ACN] = 2.0×10^{-2} and 2.0×10^{-1} M, together with calculated values employing eq 7, Φ_R^{calc}, at [ACN] = 2.0×10^{-1} M.

yields for the dimerization, Φ_R, and the *cisoid/transoid* ratio of **1** were determined at varying [TCNE]. Figure 3 plots Φ_R and the *cisoid/transoid* ratio of **1**, determined by GC on 435.8 nm irradiation of ACN against [TCNE] in DCE and AN. At low concentration of ACN ([ACN] = 1.0×10^{-3} M), the Φ_R values steeply increased as [TCNE] increased from 0 to 1.0×10^{-3} M (Figure 3a). For example, upon addition of 1.0×10^{-3} M TCNE to ACN in DCE, Φ_R jumped nearly 3-fold from 1.4×10^{-3} to 3.6×10^{-3}. On further increase of [TCNE], however, Φ_R approached a plateau of $\cong 4.1 \times 10^{-3}$. On the other hand, at high [ACN] ([ACN] = 2.0×10^{-2} and 2.0×10^{-1} M), the Φ_R values decreased as [TCNE] increased from 0 to 5.0×10^{-2} M (Figure 3b). However, higher [ACN] gives higher Φ_R than lower [ACN], and this trend is particularly remarkable when [TCNE] < 1.0×10^{-2} M. Similar trend was observed in AN. Thus, with increase of [TCNE], the Φ_R increased to a plateau ($\cong 3.4 \times 10^{-3}$) at low [ACN] condition but decreased to approach a constant value at high [ACN].

The *cisoid/transoid* ratio increased rapidly with increase of [TCNE] to give a nearly plateau value at both low (Figure 3a) and high (Figure 3b) [ACN], which is higher for higher [ACN]. Especially at low [ACN] this trend is similar to the increase of Φ_R with [TCNE] (Figure 3a). Thus, the *cisoid/transoid* ratio rapidly increased on addition of TCNE to attain a plateau of $\cong$4.6 and $\cong$6.5 in DCE and AN, respectively.

Scheme 4

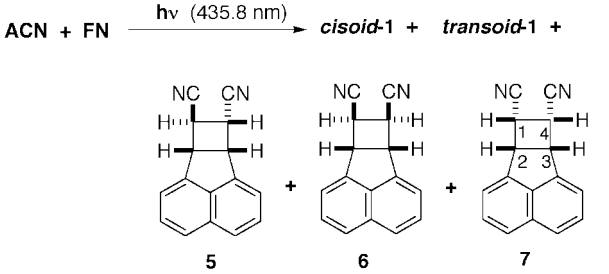

Photochemical Reaction of ACN with FN. To examine the effect of electron-accepting capability of TCNE, FN, a weaker electron acceptor with $E_{1/2}^{Red}$ of −1.36 V (vs SCE in AN),[39] has been used in place of TCNE.

The free energy change, ΔG_{ET},[40] for ET from the excited singlet state of ACN to these acceptors can be calculated according to eq 2 with values of oxidation potential ($E_{1/2}^{Ox}$) as 1.58 V[41] (vs SCE in AN) and excitation energy (ΔE_{excit}) as 257 kJ mol^{-1} [41b,c,42] for ACN.

$$\Delta G_{ET} = F[E_{1/2}^{Ox}(D) - E_{1/2}^{Red}(A)] - \Delta E_{excit} + \Delta E_{Coulomb} \quad (2)$$

Here, $\Delta E_{Coulomb}$ represents Coulomb energy between the resulted radical ions. The calculated ΔG_{ET} on direct excitation of ACN is −118.3 and −132.0 kJ mol^{-1} for TCNE and 28.4 and 14.6 kJ mol^{-1} for FN in DCE and AN, respectively. Therefore, the ΔG_{ET} value from ACN to FN is slightly positive, but highly negative from ACN to TCNE.

When ACN was mixed with FN in solution, no characteristic coloration due to development of the CT complex was observed even in a polar solvent such as AN. Absorption spectrum of this solution corresponds to the sum of the spectrum of ACN and FN. Therefore, in contrast to the ACN−TCNE system, ACN and FN do not form a CT complex in the solvents used.

On irradiation of a solution containing ACN and FN in DCE with light of >400 nm, three products were isolated in addition to the two dimers (*cisoid*-**1** and *transoid*-**1**). On the basis of EI-MS, elemental analysis, and ^{1}H NMR spectrometry, these products are identified as three isomeric [2 + 2]-cycloadducts (**5**−**7**) between ACN and FN (Scheme 4). Other products, such as the [2 + 2 + 2]-cycloadducts, were not found. The configuration at positions 1−4 of **7** was unambiguously determined by X-ray crystallography of a single crystal. The crystallographic data for this compound are summarized

(39) (a) Iwai, K.; Takemura, F.; Furue, M.; Nozakura, S. *Bull. Chem. Soc. Jpn.* **1984**, *57*, 763−767. (b) Kemp, T. J.; Parker, A. W.; Wardman, P. *J. Chem. Soc., Perkin Trans. 2* **1987**, 397−403.

(40) (a) Rehm, D.; Weller, A. *Israel J. Chem.* **1970**, *8*, 259−271. (b) Leonhardt, H.; Weller, A. *Ber. Bunsen-Ges. Phys. Chem.* **1963**, *67*, 791−795.

(41) (a) Tanimoto, I.; Kushioka, K.; Maruyama, K. *Bull. Chem. Soc. Jpn.* **1979**, *52*, 3586−3591. (b) Santa Cruz, T. D.; Akins, D. L.; Birke, R. L. *J. Am. Chem. Soc.* **1976**, *98*, 1677−1682. (c) Siegel, T. M.; Mark, H. B., Jr. *J. Am. Chem. Soc.* **1972**, *94*, 9020−9027.

(42) Levanon, H.; Neta, P.; Trozzolo, A. M. *Chem. Phys. Lett.* **1978**, *54*, 181−185.

Table 3. Product Distribution on Direct Irradiation of ACN with Light of Longer Wavelength than 400 nm in the Presence of FN in DCE and AN

			yield (%)[a]					
[ACN] (M)	[FN] (M)	solvent	*cisoid*-**1**	*transoid*-**1**	*cisoid/transoid*	**5**	**6**	**7**
1.0×10^{-3}	1.0×10^{-3}	DCE	25	39	0.64			
1.0×10^{-2}	1.0×10^{-2}	DCE	30.2	34.3	0.88	8.8	7.8	5.9
5.0×10^{-2}	5.0×10^{-2}	DCE	35.8	26.0	1.41	6.9	4.0	4.8
2.0×10^{-1}	2.0×10^{-1}	DCE	17.2	11.5	1.50	1.1	t[b]	1.0
1.0×10^{-3}	1.0×10^{-3}	AN	44	22	2.00			
1.0×10^{-2}	1.0×10^{-2}	AN	48.3	24.2	1.99	4.8	6.5	5.4
5.0×10^{-2}	5.0×10^{-2}	AN	45.0	11.9	3.94	3.3	3.1	3.0
2.0×10^{-1}	2.0×10^{-1}	AN	14.3	3.1	4.60	t[b]	1.3	0.9

[a] Yields determined by means of ^{1}H NMR based on consumed ACN. Conversion of ACN is 45−85%. [b] Trace.

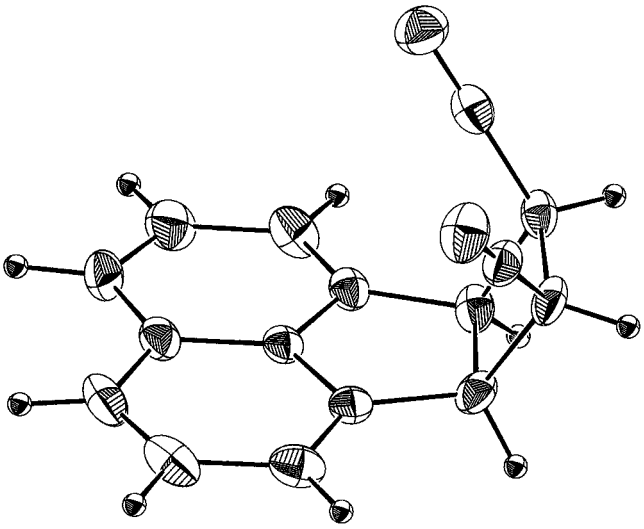

Figure 4. ORTEP drawing of compound **7**.

in Table 1. The ORTEP diagram in Figure 4 shows the structure of **7**, where both pairs of protons (H_1 and H_4, H_2 and H_3) are cis and two protons (H_2 and H_3) are aligned as anti with the two cyano groups. The structures of **5** and **6** are established on the basis of comparison of their ^{1}H NMR spectra with that of **7**. Thus, three equivalent pairs of aromatic protons, two equivalent aliphatic tertiary protons, and a smaller J_{1-2} value than that of **7** support the structure for **6**. Similarly, the nonequivalent six aromatic protons and the nonequivalent aliphatic tertiary protons support the structure for **5**.

Yields of the above products obtained in various concentrations of ACN and FN in DCE and AN are shown in Table 3. In each case, formation of *cisoid*-**1** and *transoid*-**1** prevails over that of **5**−**7**. Addition of FN slightly increased the *cisoid*/*transoid* ratio, but the effect was not so remarkable in addition of TCNE. No selectivity among **5**−**7** was noted.

Quantum yields (Φ_R) of the dimerization of ACN were determined in varying [FN] on irradiation of 435.8 nm light. Figure 5 plots Φ_R and the *cisoid*/*transoid* ratio against [FN] in DCE and AN. Both Φ_R and the *cisoid*/*transoid* ratio are almost insensitive to [FN] at low (Figure 5a) and high (Figure 5b) [ACN]. This means that the addition of FN does not affect the dimerization of ACN, which is quite in contrast to the ACN−TCNE system (Figure 3).

Preparation of a Crystalline CT Complex of ACN with TCNE and Its Irradiation in the Solid State.[43] An equimolar solution of ACN and TCNE were mixed in ethyl acetate, and the mixture was slowly evaporated at

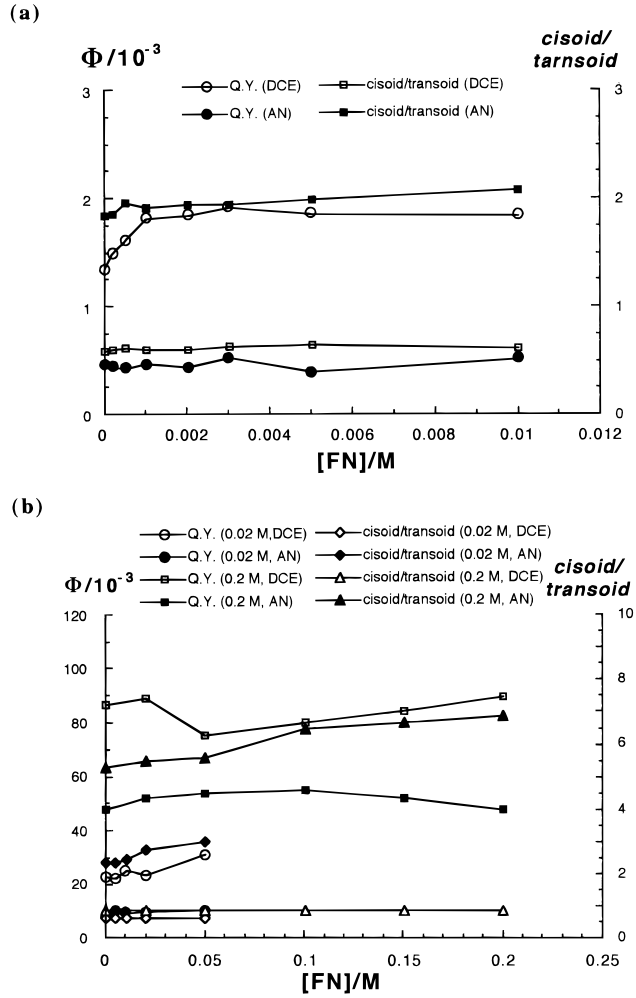

Figure 5. Plots of quantum yield (Q.Y.) for photodimerization of ACN, Φ_R, and the *cisoid*/*transoid* ratio versus [FN] in DCE and AN: (a) [ACN] = 1.0×10^{-3} M; (b) [ACN] = 2.0×10^{-2} and 2.0×10^{-1} M.

ambient temperature to give a crystalline 1:1 CT complex between ACN and TCNE (ACN·TCNE), as tan-brown cubes, mp 103.0−105.0 °C. The 1:1 composition and purity of the crystalline CT complex were satisfactorily verified by elemental analysis. From the X-ray crystallographic analysis, as listed in Table 1, the crystalline CT complex is monoclinic and belongs to the space group of $P2_1/n$. Figure 6a shows the molecular packing in ACN·TCNE along the *a* axis. One-dimensional columns of ACN·TCNE are constituted along this axis, where ACN and TCNE are stacked alternately. Molecular arrangement in the crystal viewed along the *b* axis is shown in

Table 4. Product Distribution of Photochemical Reactions of ACN in the Solid State

			yields (%)[a]					
substrate	state	*hν* (nm)	temp (°C)	conversion (%)	*cisoid*-**1**[b]	*transoid*-**1**[b]	cisoid/transoid	**2**[c]
ACN	crystal	>400	25	14.5	15.8	83.2	0.19	
ACN·TCNE	crystal	>500	25	25.4	0	0		80.7
ACN·TCNE	crystal	>500	−10	26.9	0	0		78.2
ACN·TCNE	crystal	>400	25	38.5	0	0		73.3
ACN·TCNE	mixed powder	>500	25	30.6	5.2	7.3	0.71	75.8
ACN·TCNE	mixed powder	>400	25	52.5	13.1	65.6	0.20	12.2

[a] Yields based on **1** recovered. [b] Determined by GC. [c] Isolated by flash column chromatography.

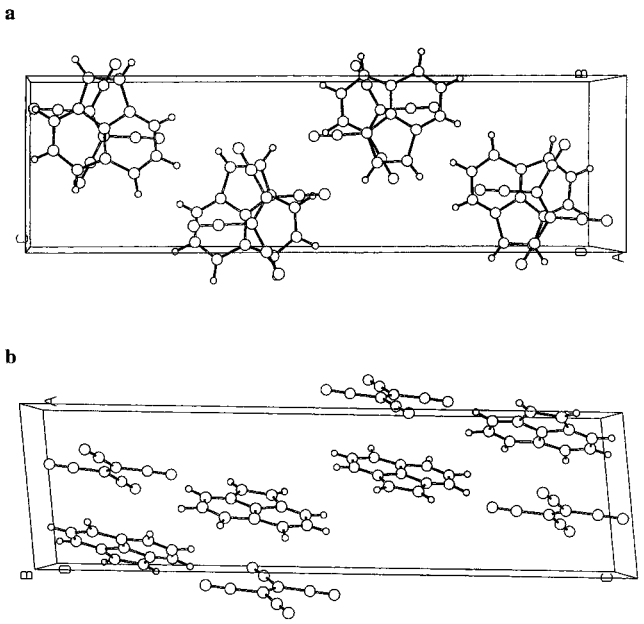

Figure 6. Molecular arrangement in the crystalline ACN·TCNE along the *a* axis (a) and the *b* axis (b).

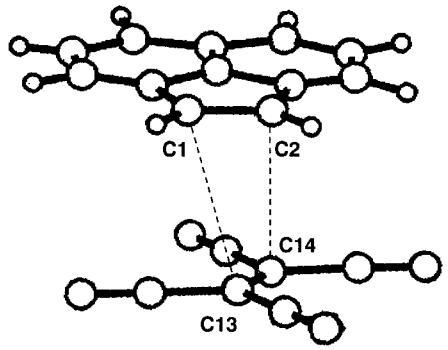

Figure 7. Molecular pair in the crystalline ACN·TCNE.

Figure 6b. One unit cell consists of four columns, in which two ACN·TCNE molecules are included. Two molecules of ACN in the adjacent columns in a same lattice are aligned in parallel and face the opposite direction. A pair of ACN·TCNE is given in Figure 7. The dihedral angle between the plane of ACN and TCNE in the crystal is 0.8° with a torsion angle between two alkene parts of ACN and TCNE of 62.2°.

ACN·TCNE was irradiated with >500-nm light under argon atmosphere at 25 °C. Surprisingly enough, under this CT excitation condition, photochemical reaction between ACN and TCNE took place to give **2** as a sole product without giving any other products such as *cisoid*-**1**, *transoid*-**1**, **3**, and **4**.[43] For example, on irradiation of ACN·TCNE for 7.0 h, 25.0% of ACN·TCNE was converted into **2** in 80.7% yield (based on consumed ACN) determined by chromatographic isolation (Table 4). This is in contrast to CT excitation in solutions which did not result in any net photochemical reaction. The quantum yield for formation of **2** was ca. 4 (±1) × 10^{-3} under irradiation of 546.1 nm monochromatic light. This solid-state reaction was not affected by reaction temperature (−10−25 °C). Wavelength of the irradiation light essentially did not affect the reaction except that we obtained higher yields of **2**. When the crystalline CT complex was irradiated with light > 400 nm, **2** was formed in a 73.2% yield with a conversion of 38.5%, which is in contrast to the irradiation in solutions giving five products in appropriate yields (Table 2). For comparison, a single crystal of ACN was irradiated (λ > 400 nm) at 25 °C to give *cisoid*-**1** and *transoid*-**1** with the *cisoid*/*transoid* ratio of 0.19.

To compare the behavior of the crystalline CT complex in a topochemically ordered crystal lattice with that in the solid state where molecules randomly arrange, irradiation of a ground powder of a mixture of ACN and TCNE was examined. Thus, an equimolar mixture of ACN and TCNE was pulverized in a mortar, and the resulted tan-brown-colored fine powder was irradiated under the same conditions as in the case of ACN·TCNE. As included in Table 4, irradiation of the mixed powder with >500 nm light afforded **2** accompanied by lesser amounts of *cisoid*-**1** and *transoid*-**1** with the *cisoid*/*transoid* ratio of 0.71. The above *cisoid*/*transoid* ratio of the dimer is much larger than that of the irradiation of ACN crystal without TCNE and those reported by Cohen et al.[44] and Livingston and Wei.,[45] who described *transoid*-**1** as the sole product at 20 °C. It is noteworthy that direct excitation of ACN in the mixed powder with >400-nm light resulted in decrease of **2** and instead increase of **1** with the *cisoid*/*transoid* ratio of 0.20, which is close to that for the direct irradiation of ACN crystal without TCNE (Table 4). Formation of **3** and **4** was not observed in the solid-state irradiation.

Discussion

(a) SSIP Mechanism for the Dimerization of ACN. Direct excitation of ACN in solution in the presence of TCNE gave not only *cisoid*-**1** and *transoid*-**1** but also **2**−**4**. As we discuss below, TCNE works as an electron acceptor to either the singlet or the triplet excited state of ACN to give a singlet or triplet solvent-separated radical ion pair (SSIP) particularly at high or low [ACN], respectively; among them the singlet radical ion pair (singlet

(43) Haga, N.; Nakajima, H.; Takayanagi, H.; Tokumaru, K. *Chem. Commun.* **1997**, 1171−1172.
(44) Cohen, M. D.; Ron, I.; Schmidt, G. M. J.; Thomas, J. M. *Nature* **1969**, *224*, 167−168.
(45) Wei, K. S.; Livingston, R. *J. Phys. Chem.* **1967**, *71*, 548−549.

Scheme 5

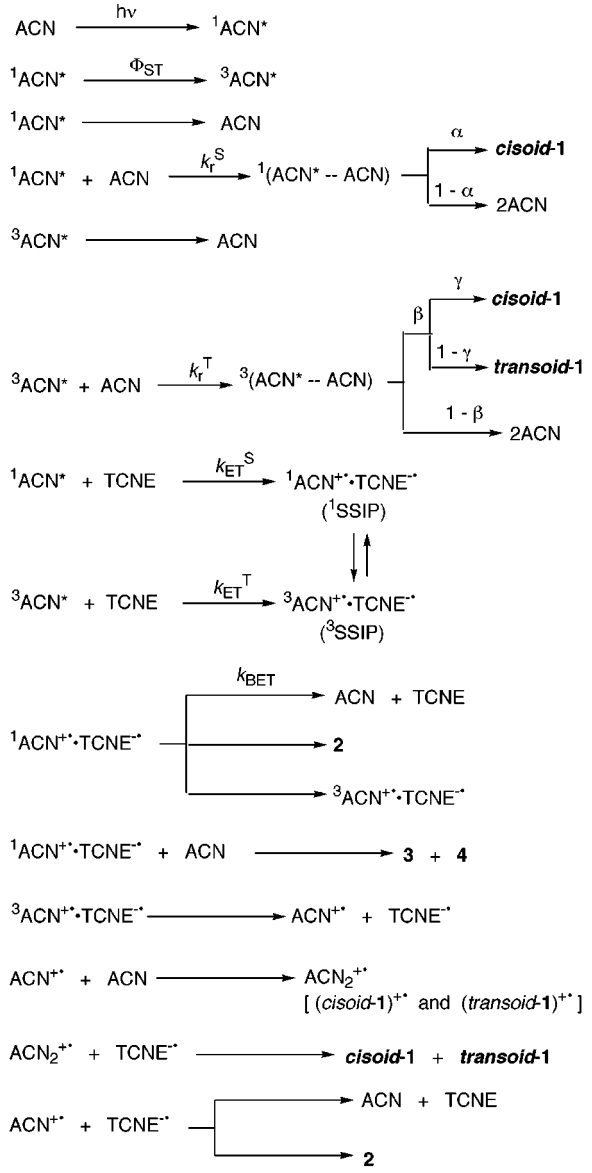

SSIP) mostly undergoes BET preceding diffusion probably through the triplet SSIP, but the triplet SSIP undergoes diffusion to give the radical ion pair $ACN^{+\bullet}$ and $TCNE^{-\bullet}$. Then $ACN^{+\bullet}$ adds to ACN to give $ACN_2^{+\bullet}$, which will react with $TCNE^{-\bullet}$ to afford **1** or reacts with $TCNE^{-\bullet}$ to give the 1:1 cycloadduct **2**. The mechanism for the reaction is depicted in Scheme 5 and briefly in Scheme 6. The present mechanism well fits the various observation, particularly the effect of [ACN] and [TCNE] or the Φ_R and the *cisoid*/*transoid* ratio of **1** as described below.

First, we discuss the effect of [TCNE] on the Φ_R and the *cisoid*/*transoid* ratio when [ACN] is low such as 1.0×10^{-3} M. When [ACN] = 1.0×10^{-3} M, both Φ_R and the *cisoid*/*transoid* ratio steeply increase with increase of [TCNE] to attain a plateau value (Figure 3a). Thus, addition of TCNE enhances production of **1**, accompanying the increase of its *cisoid*/*transoid* ratio. In the absence of TCNE, as we have previously reported, at [ACN] = 1.0×10^{-3} M, Φ_{ST} (0.18 in DCE and 0.029 in AN) is much larger than the quantum yield for the dimerization from the S_1 state, Φ_R^S (5.7×10^{-4} in DCE and 2.8×10^{-4} in AN).[21] Therefore, at low [ACN] ET to TCNE will proceed from the T_1 state. Thus, the T_1 state will either add to the ground-state ACN with a rate constant of k_r^T collapsing to *cisoid*-**1** and *transoid*-**1** with an efficiency of β or undergo ET to TCNE with a rate constant of k_{ET}^T to give a triplet radical ion pair of $ACN^{+\bullet}$ and $TCNE^{-\bullet}$ leading to *cisoid*-**1** and *transoid*-**1** with an efficiency of x_T competing with deactivation with a lifetime, τ_T. Then the Φ_R is given by eq 3.

$$\Phi_R = \Phi_{ST} \frac{k_r^T[ACN]\beta + k_{ET}^T[TCNE]x_T}{\tau_T^{-1} + k_r^T[ACN] + k_{ET}^T[TCNE]} \quad (3)$$

When [TCNE] is sufficiently high, ET from the T_1 state to TCNE will proceed much faster than deactivation and addition to the ground-state ACN (k_r^T of 2.1×10^6 and 2.6×10^6 M^{-1} s^{-1} and τ_T of 2.9×10^{-6} and 2.2×10^{-6} s in DCE and AN,[14e,21] respectively). Accordingly, eq 3 can be approximated as eq 4.

$$\Phi_R = \Phi_{ST}x_T \quad (4)$$

Equation 4 means that, under the above conditions, where the dimerization occurs from $ACN^{+\bullet}$, the Φ_R attains a plateau value, $\Phi_{ST} \cdot x_T$. This satisfactorily agrees with the results in Figure 3a. Based on the plateau Φ_R value at 2.0×10^{-3} M TCNE, 0.0040 in DCE and 0.0035 in AN, x_T can be obtained as 0.023 and 0.11 in DCE and AN, respectively (Table 5). More than 5 times lower x_T value in DCE than that in AN may reflect more facile reversion of the triplet SSIP to the singlet one in DCE than in AN probably due to the heavy atom effect of chlorine atoms of DCE. The *cisoid*/*transoid* ratio of **1** observed as a plateau value at high [TCNE], 4.5 and 6.2 in DCE and AN, respectively, corresponds to the *cisoid*/*transoid* ratio of the dimer formed from $ACN^{+\bullet}$.

At low [TCNE] ($<1.0 \times 10^{-3}$ M), where the T_1 state predominantly undergoes unimolecular deactivation, k_r^T[ACN] and k_{ET}^T[TCNE] in the denominator of eq 3 are much smaller than τ_T and can be neglected. Also k_r^T[ACN]β in the numerator can be omitted. Therefore, the Φ_R increases linearly with [TCNE] at low [TCNE] as in eq 5. From the linear relation between Φ_R and [TCNE]

$$\Phi_R = \Phi_{ST}\tau_T k_{ET}^T[TCNE]x_T \quad (5)$$

at the low [TCNE] in Figure 3a, one can obtain $\tau_T\Phi_{ST}k_{ET}^Tx_T$ as a slope. On the basis of the slope (2.09 and 2.39 M in DCE and AN, respectively) and the data in Table 5, k_{ET}^T was determined as 2.3×10^8 and 3.4×10^8 M^{-1} s^{-1} in DCE and AN. The obtained k_{ET}^T values are 100 times smaller than the diffusion-controlled rate constant. This may be due to activation energy for ET from the T_1 state of ACN to TCNE, though the triplet state of ACN (179−181 kJ mol^{-1})[46] lies higher in energy than that of the SSIP (121 kJ mol^{-1}).

Second, we discuss the effect of [TCNE] at high [ACN]. On the contrary to the acceleration of the dimerization by TCNE at low [ACN], at higher [ACN] (2.0×10^{-1} and 2.0×10^{-2} M), increase of [TCNE] reduces the Φ_R to an almost constant value (Figure 3b) but increases the *cisoid*/*transoid* ratio to get a near plateau similar to at low [ACN] when [ACN] is as high as 1.0×10^{-1} M. This suppression of dimerization by added TCNE is not due

(46) Kobashi, H.; Ikawa, H.; Kondo, R.; Morita, T. *Bull. Chem. Soc. Jpn.* **1982**, *55*, 3013−3018.

Scheme 6

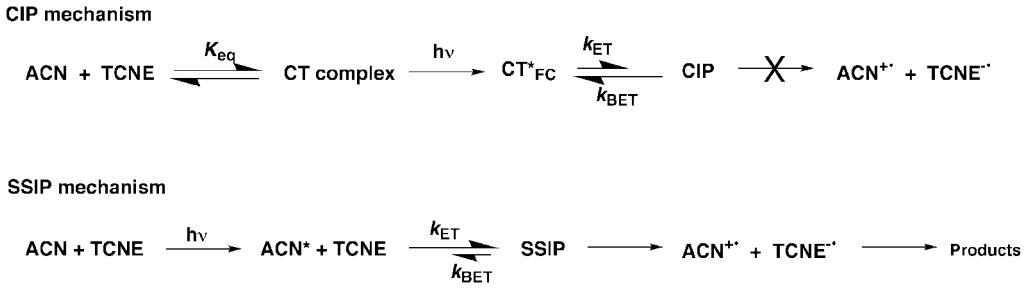

Table 5. Various Kinetic Data and Quantum Yields for Intersystem Crossing Relating to the Dimerization of ACN in the Presence of TCNE

	DCE	AN
α^a	0.257	0.286
k_r^S (M^{-1} s^{-1})^a	6.3×10^9	2.6×10^9
$\beta^{a,b}$	0.85	1.05
$\Phi_{ST}{}^a$	0.18	0.029
k_r^T (M^{-1} s^{-1})^{a,c}	2.13×10^6	1.78×10^6
τ_T (s)^{a,c}	2.93×10^{-6}	2.24×10^{-6}
$\gamma^{a,c}$	0.337	0.618
k_{ET}^T (M^{-1} s^{-1})	2.3×10^8	3.4×10^8
k_{ET}^S (M^{-1} s^{-1})	3.3×10^{11}	5.8×10^{11}
x_T	0.023	0.11
x_S	0.017	0.015

[a] From ref 21. [b] Determined by Eosin-Y-sensitized reaction on irradiation at 546.1 nm. [c] Determined by quenching with ferrocene.

to increase of proportion of the CT complex. For example, at [ACN] = 2.0×10^{-1} M in AN, increase of [TCNE] from 0 to 1.0×10^{-3}, 1.0×10^{-2}, and 5.0×10^{-2} M reduced the Φ_R from 0.048 to 0.027, 0.016, and 0.015, whereas nearly 20% out of total ACN formed the CT complex in each case. Therefore, decrease of free ACN by forming the CT complex, which is inert for photochemical reactions, cannot be ascribed to this suppression of dimerization.

At low [ACN], the active excited state is the T_1 state of ACN as described above. On the other hand, at high [ACN], as reported previously,[21] in the absence of TCNE, the singlet state of ACN can add to ACN competing with deactivation to the ground state and to the triplet state. For simplicity, let us assume the suppression of Φ_R with TCNE as quenching of the dimerization from the S_1 state by TCNE; TCNE quenches the S_1 state and will give a singlet SSIP, which will subsequently undergo facile BET without giving net products. Then, the ratio of the quantum yields in the absence of TCNE, $\Phi_R{}^0$, to that in the presence of TCNE, $\Phi_R{}^{TCNE}$, is represented by eq 6, where τ_s, k_r^S, and k_{ET}^S stand for the singlet lifetime, rate constant for addition of the S_1 state to the ground state of ACN, and rate constant for quenching of the S_1 state by TCNE by ET, respectively.

$$\frac{\Phi_R{}^0}{\Phi_R{}^{TCNE}} = 1 + \frac{k_{ET}{}^S[TCNE]}{\tau_S{}^{-1} + k_r{}^S[ACN]} \qquad (6)$$

Figure 8 presents typical Stern−Volmer plots for [ACN] = 2.0×10^{-1} M in DCE and AN, which afford a linear relationship with an intercept close to unity. The observed slope is 81.3 in DCE and 174.7 M^{-1} in AN. Applying τ_s^{-1} of 2.8×10^8 s^{-1} [17,18] and k_r^S of 6.3×10^9 and 2.6×10^9 M^{-1} s^{-1} in DCE and AN,[21] k_{ET}^S value can be given as 3.3×10^{11} and 5.8×10^{11} M^{-1} s^{-1} in DCE and AN, respectively, though these values are higher

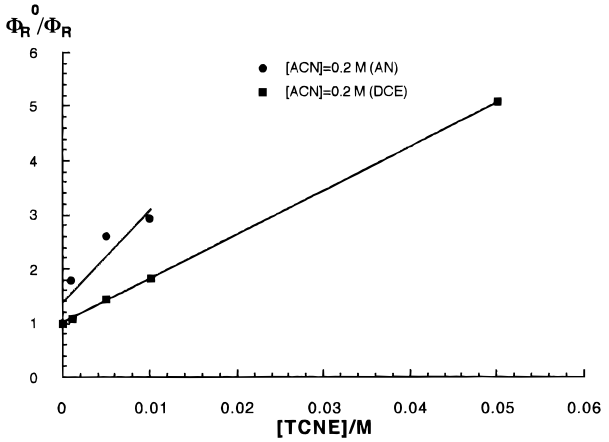

Figure 8. Stern−Volmer plots for quenching of the photodimerization of ACN by TCNE at [ACN] of 2.0×10^{-1} M.

than those commonly accepted for ET probably due to very simplified treatment of the data.

Generally, at high [ACN] four pathways can give **1**, that is, dimerization of ACN from the S_1 and T_1 states without ET, and via ET from the S_1 and T_1 states to TCNE (Scheme 5). The S_1 state undergoes ET to TCNE with a rate constant k_{ET}^S, and the resulting SSIP collapses to the products with an efficiency of x_S. The quantum yield for the dimerization (Φ_R) at high [ACN] is given in eq 7. At high [TCNE], the S_1 state is assumed

$$\Phi_R = \frac{k_r{}^S[ACN]\alpha + k_{ET}{}^S[TCNE]x_S + \Phi_{ST}\left(\dfrac{k_r{}^T[ACN]\beta + k_{ET}{}^T[TCNE]x_T}{\tau_T{}^{-1} + k_r{}^T[ACN] + k_{ET}{}^T[TCNE]}\right)}{\tau_S{}^{-1} + k_r{}^S[ACN] + k_{ET}{}^S[TCNE]} \qquad (7)$$

to undergo ET to TCNE with a rate constant much larger than that for the addition to the ground-state ACN. Furthermore, ET from the S_1 state to TCNE must be sufficiently faster than deactivation of the S_1 state when [TCNE] > 1.0×10^{-2} M. Then, at high [TCNE], eq 7 can be simplified as eq 8. At high [TCNE], the first term

$$\Phi_R = \frac{k_r{}^S[ACN]\alpha + \Phi_{ST}x_T}{k_{ET}{}^S[TCNE]} + x_S \qquad (8)$$

in eq 8 can be neglected ($k_{ET}^S[TCNE] \gg k_r^S[ACN]\alpha + \Phi_{ST}x_T$). Hence, Φ_R is to be reduced to a nearly constant value with increase of [TCNE], which agrees with the results in Figure 3b. On the basis of Φ_R values, x_S can be determined from eq 8 as 0.017 and 0.015 in DCE and AN, respectively. These data are collected in Table 5.

As to x_S and x_T, the fractions of the S_1 and T_1 states of ACN quenched with TCNE leading to dimerization, respectively, in AN x_T is nearly 10 times larger than x_S. This will reflect the difference of the nature of the resulting triplet and singlet SSIP of $ACN^{+\bullet}$ and $TCNE^{-\bullet}$. On the other hand, in DCE x_T is no more than twice of x_S. This may reflect the heavy atom effect of chlorine atoms in DCE as mentioned before.

Using eq 7, Φ_R values at various [TCNE] can be calculated, and the calculated values, Φ_R^{calc}, are included in Figure 3b. As Figure 3b indicates, plots for Φ_R^{calc} satisfactorily agree well with those for the observed Φ_R. This substantiates the validity of the mechanism shown in Scheme 5. The opposite effect of TCNE on Φ_R at between low and high [ACN], that is, to increase Φ_R at low [ACN] but to reduce Φ_R at high [ACN], is reasonably attributed to difference of efficiency to give product from the singlet SSIP, x_S, and from the triplet SSIP, x_T. Thus, at low [ACN] ET to TCNE exclusively proceeds from the T_1 state, which gives the products in relatively high efficiency ($x_T = 0.023$ and 0.11 in DCE and AN, respectively), due to relatively slow BET from the triplet SSIP. On the other hand, at high [ACN] ET mainly proceeds from the S_1 state which gets to the products with low efficiency ($x_S = 0.017$ and 0.015 in DCE and AN, respectively) because of faster BET from the singlet SSIP. Therefore, at high [ACN], TCNE functions as a quencher of the S_1 state rather than an effective reactant.

Variation of the *cisoid*/*transoid* ratio of **1** with [TCNE] in DCE is similar at high [ACN] and at low [ACN] affording a plateau value of 5.0 (Figure 3). This indicates that both the singlet and the triplet SSIP give **1** in the same *cisoid*/*transoid* ratio in DCE. This again suggests that in DCE the singlet SSIP will easily convert to the triplet SSIP, subsequently undergoing diffusion to give free $ACN^{+\bullet}$, which then reacts with ACN finally affording *cisoid*-**1** and *transoid*-**1** in a ratio of 5.0. On the other hand, in AN the *cisoid*/*transoid* ratio attained at high [TCNE] is higher at high [ACN] (11) than at low [ACN] (6.2). The reason for this difference is not clear. However, one could suppose that an $ACN^{+\bullet}$ site in a singlet SSIP might interact with an ACN molecule out of the pair with *cisoid*-type configuration leading to a cage-wall cycloaddition as suggested for photocycloaddition between two molecules of 1,1-diphenylethylene sensitized with 9,10-dicyanoanthracene.[8a]

The dissociated $ACN^{+\bullet}$ from the singlet or triplet SSIP reacts with the ground-state ACN to give a dimeric radical cation, $ACN_2^{+\bullet}$ (Scheme 5). The $ACN_2^{+\bullet}$ can take *cisoid*- and *transoid*-type configuration corresponding to $(cisoid\text{-}\mathbf{1})^{+\bullet}$ and $(transoid\text{-}\mathbf{1})^{+\bullet}$. Therefore, the stereochemistry of the resulting **1** will be determined when $ACN^{+\bullet}$ adds to ACN. Charge recombination between $ACN_2^{+\bullet}$ and $TCNE^{-\bullet}$ gives *cisoid*-**1** and *transoid*-**1** in a *cisoid*/*transoid* ratio depending on the solvents used.

Why does formation of *cisoid*-**1** notably prevail over formation of *transoid*-**1** in the radical cation mechanism? Generally speaking, in the case of photodimerization of alkenes proceeding via ET mechanism, little consistency has been observed for stereoselectivity for the dimeric products.[5−10] It is worth noting that photochemically generated radical cations of some 1,3-diarylpropanes, i.e., 1,3-dinaphthylpropane, 1,3-dipyrenylpropane, and 1,3-dicarbazolylpropane, are stabilized in a sandwich-like overlap conformation of the two aryl chromophores.[47] The same goes for dimeric radical cations in poly(vinylpyrenes) generated by pulse radiolysis.[48] This attractive force, which is defined as charge-resonance energy,[49] is estimated as several kilocalories per mole in magnitude from their charge-resonance band. The present results indicate that addition of $ACN^{+\bullet}$ to ACN gives $(cisoid\text{-}\mathbf{1})^{+\bullet}$ several times more efficiently than $(transoid\text{-}\mathbf{1})^{+\bullet}$, since in the former the two naphthyl chromophores can adopt a somewhat parallel sandwich-like conformation and can exert an attractive interaction to delocalize the positive charge to stabilize this species.

The plateau Φ_R value for the dimerization in the presence of TCNE, which is much smaller than unity, may rule out a chain reaction mechanism which proceeds by the way of ET from the ground-state ACN to $ACN_2^{+\bullet}$ giving $ACN^{+\bullet}$ and **1** (*cisoid* or *transoid*), though $E_{1/2}^{Ox}$ for *cisoid*-**1** (1.98 V[50] vs SCE in AN) is higher than that for ACN (1.58 V[41] vs SCE in AN).

(b) Formation of 2−4 from $ACN^{+\bullet}$. Excitation of ACN in the presence of TCNE afforded **2**−**4** besides the dimers (*cisoid*-**1** and *transoid*-**1**). Formation of **2** from irradiation of ACN in the presence of TCNE in DCE with light of >300 nm was previously reported by Shirota et al.[22]

In the present reaction, **3** and **4** were produced only when [ACN] was as high as 1.0×10^{-1} M and [TCNE] was higher than 1.0×10^{-2} M. If **3** and **4** were produced by reaction between $ACN_2^{+\bullet}$ and $TCNE^{-\bullet}$, this process should take place even at low [ACN] competing with production of *cisoid*- and *transoid*-**1** by charge recombination between these species. Therefore, the present results suggest a possible mechanism in which an ACN molecule can interact with a singlet SSIP to give **3** and **4** particularly at high [ACN]; the stationary concentration of the SSIP will be sufficiently high at high [TCNE] for the above reaction to occur. High [ACN] will be effective to undergo addition to ACN in the SSIP. Furthermore, production of **3** and **4** at a slight expense of production of **2** with increase of [TCNE] suggests that **2** also can result from geminate reaction in the SSIP as well as from coupling of free $ACN^{+\bullet}$ and $TCNE^{-\bullet}$.

(c) Photochemical Inertness of CT Complex of ACN−TCNE in Solutions (CIP Mechanism). The tan-brown coloration observed immediately after mixing solutions of ACN and TCNE shows formation of a CT complex between ACN and TCNE in the ground state. The intensity of the color increases with increase of the initial concentration of ACN and TCNE as shown in Figure 1, obeying eq 1 for complex formation with the 1:1 stoichiometry in Scheme 2.

Selective excitation of the CT complex with light of >500 nm did not result in any reaction in contrast to excitation of ACN with >400-nm light in the presence of TCNE in solution. Excitation of a CT complex generally

(47) (a) Washio, M.; Tagaya, S.; Tabata, Y. *Polym. J.* **1981**, *13*, 935−938. (b) Tsuchida, A.; Tsujii, Y.; Ito, Y.; Yamamoto, S. *J. Phys. Chem.* **1989**, *93*, 1244−1248. (c) Tsujii, Y.; Tsuchida, A.; Onogi, Y.; Yamamoto, M. *Macromolecules* **1990**, *23*, 4019−4023. (d) Tsuchida, A.; Tsujii, Y.; Ohoka, M.; Yamamoto, M. *J. Phys. Chem.* **1991**, *95*, 5797−5802. (e) Tsuchida, A.; Yamamoto, M. *J. Photochem. Photobiol. A: Chem.* **1992**, *65*, 53−59.

(48) Tsuchida, A.; Ikawa, T.; Yamamoto, M.; Ishida, A.; Takamuku, S. *J. Phys. Chem.* **1995**, *99*, 14793−14797.

(49) Yamamoto, M.; Tsujii, Y.; Tsuchida, A. *Chem. Phys. Lett.* **1989**, *154*, 559−562.

(50) Haga, N. Unpublished results.

Scheme 7

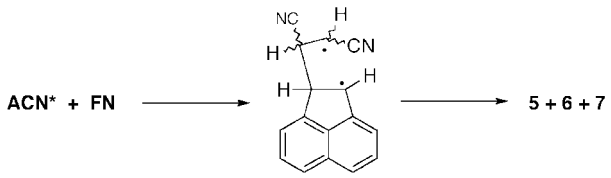

8

gives a contact RIP (CIP).[23−25] In some donor−acceptor systems, BET proceeds much faster from CIP than SSIP as observed by transient absorption spectroscopy using femtosecond laser photolysis.[25] The present result indicates that the resulting CIP very rapidly undergoes BET preceding dissociation to free radical ions through SSIP. This is attributed to a very low net energy for BET, as low as 1.34 V, since CIP is known to undergo rapid BET particularly when the CIP lies very close in energy to the ground state.[25] According to Miyasaka et al., CIP with a $-\Delta G_{BET}$ of around 1.34 V quickly deactivates with a rate constant of 10^{11} s^{-1}.[24] The mechanism involving CIP formed by excitation of the CT complex rationalizes this phenomenon (Scheme 5).

Distinction of reactivity and product distribution between selective CT excitation and bimolecular quenching has been observed for the photoreduction of chloranil by acenaphthene.[51] Jones et al. rationalized this distinction in terms of spin multiplicity of the resulted radical ion pair.

(d) Reaction of ACN with FN. As shown in Figure 5, on irradiation of ACN with FN both Φ_R and the *cisoid*/*transoid* ratio for the dimerization do not increase with increase of [FN]. Dimerization of ACN seems to proceed irrespective of the presence of FN. This is quite in contrast to those in the presence of TCNE. The above results indicate that the radical ions, $ACN^{+\bullet}$ and $FN^{-\bullet}$, do not participate in the dimerization. This reflects that ET from the S_1 state of ACN to FN is endergonic as described before.

Furthermore, formation of the [2 + 2 + 2]-cycloadducts of ACN and FN was not observed, whereas the corresponding products (**3** and **4**) were isolated on direct irradiation of ACN in the presence of TCNE. This again shows no participation of $ACN^{+\bullet}$ and $ACN_2^{+\bullet}$. Alternatively, a mechanism shown in Scheme 7 involving a biradical (**8**) as an intermediate is in accord with the present outcome. Because if the excited ACN underwent addition to FN via a concerted process, **6** and **7** would never be produced.

(e) Photochemical Reaction of the Crystalline CT Complex under Topochemical Control. It is quite remarkable that CT excitation of the crystalline CT complex (ACN·TCNE) gave **2** as a sole product with a Φ_R of 4×10^{-3} in contrast to the inertness of the CT complex in solution. This is attributed to retention of proximity and rigid mobility of the ACN and TCNE molecules in the crystalline lattice (Figures 6 and 7). Thus, molecules of ACN and TCNE in the crystalline CT complex are continually held in a favorable configuration and distance for ET to take place; that is, the distance between the ACN and TCNE plane is 3.5 Å with a dihedral angle of 0.8°. Though the rate for BET from CIP is essentially fast, the retention of proximity and rigid mobility of ACN and TCNE in the crystal should retard the BET but enable the two alkenic parts to undergo cycloaddition. Moreover, the absence of solvent molecules does not stabilize the CIP, which will also retard the BET. On the other hand, in solution the excited CT complex and the CIP are solvated, tend to undergo rapid BET due to small $-\Delta G_{BET}$, will not maintain favorable configuration to undergo addition because of their mobility, and therefore result in facile deactivation or BET to the ground state.

In the crystal lattice, two alkenic parts of ACN and TCNE are aligned parallel with a torsion angle of 62.2° with the interatomic distances of C1−C13 and C2−C14 of 3.43 and 3.65 Å, respectively (Figure 7). This feature of molecular arrangement satisfies the requirements for the [2 + 2]-cycloaddition of ACN to TCNE in the solid state under the topochemical control in the crystal lattice (Schmidt's rule).[52] Another combination of the alkenic carbon atoms, C1−C14 and C2−C13 with distances of 3.97 and 3.33 Å, respectively, is also possible for the cycloaddition, which satisfies Schmidt's rule. Considering the more remote distance of C1−C14, the former combination is more favorable than the latter. Topological transformation is necessarily accompanied from the torsion angle of 62.2° between the two alkenic C═C double bonds to the parallel C−C single bond of the cyclobutane moiety in **2**. Though this movement requires unoccupied large space in the crystal lattice, significantly low density (1.268 g cm^{-3}) of the crystalline CT complex can satisfy this requirement.

Much higher reactivity of ACN on direct excitation than that by CT excitation may be the reflection of more effective ET in the crystalline CT complex due to increase of photons absorbed. In this condition, however, not only CT excitation of ACN·TCNE but also local excitation of ACN is accomplished.

In contrast to proximity of the alkenic carbons of ACN and TCNE, those of two molecules of ACN in the crystalline CT complex are aligned unfavorably for the dimerization reaction to give the dimers (*cisoid*-**1** and *transoid*-**1**) with interatomic distances longer than 6 Å. Apparently, these distances are out of order of the limit value (4.2 Å) to undergo reaction in solid state.[52] The crystal structure of ACN·TCNE is necessarily advantageous for formation of **2** and disadvantageous for *cisoid*-**1** and *transoid*-**1**. Moreover, formation of **3** and **4** in the crystalline CT complex is definitely unfavorable, because it is necessary to generate $ACN_2^{+\bullet}$, which is the common intermediate of *cisoid*-**1** and *transoid*-**1**.

It is quite suggestive to compare the photochemical behavior in the topochemically ordered crystalline CT complex with that in the randomly disordered mixed powder. Irradiation ($\lambda > 500$ nm) of the mixed powder of an equimolar mixture of ACN and TCNE afforded not only **2** but also a small amount of *cisoid*-**1** and *transoid*-**1** with a *cisoid*/*transoid* ratio of 0.71 (Table 4). A higher yield of **2** than *cisoid*-**1** and *transoid*-**1** in this condition gives evidence for formation of ACN·TCNE in high proportion by pulverization. Furthermore, the formation of *cisoid*-**1** and *transoid*-**1** indicates that a part of $ACN^{+\bullet}$ produced by CT excitation of the CT complex can add to a ground-state ACN to give $ACN_2^{+\bullet}$. A looser and more random arrangement of molecules of ACN and TCNE in

(51) (a) Jones, G., II; Haney, W. A.; Phan, X. T. *J. Am. Chem. Soc.* **1988**, *110*, 1922−1929. (b) Jones, G., II; Mouli, N.; Haney, W. A.; Bergmark, W. R. *J. Am. Chem. Soc.* **1997**, *119*, 8788−8794.

(52) Pages 133−184 in ref 32.

the mixed powder, where two molecules of ACN can be located proximately, should allow to undergo the dimerization. A much higher *cisoid*/*transoid* ratio on CT excitation than those on direct excitation of ACN in the mixed powder and on irradiation of the ACN crystal without TCNE (Table 4)[44,45] supports preferable formation of $ACN_2^{+\bullet}$ which is stabilized by charge resonance[47−49] under irradiation of >500-nm light to excite the CT complex. Absence of **3** and **4** in this condition is in accord with the requirement of enormous movement (topological transformation) of the resulting CIP to interact with the ground-state ACN in the crystalline lattice.

Formation of a lower yield of **2** and higher yields of *cisoid*-**1** and *transoid*-**1** on direct excitation of ACN in the mixed powder than on CT excitation shows contribution of addition of the S_1 or T_1 state to the ground state of ACN to production of **1** which proceeds competitively with the radical ion pathway in the mixed powder due to the loose and random structure of the mixed powder. A lower *cisoid*/*transoid* ratio of 0.20 than that in the CT excitation, which is close to that for the dimerization in the topochemically controlled crystal of ACN in the absence of TCNE (Table 4),[44,45] clearly indicates that the excited state of ACN adds to ACN in these conditions.

Conclusions

This work has revealed unique features of photoinduced ET and the behavior of the resulting radical ions ($ACN^{+\bullet}$ and $TCNE^{-\bullet}$) in the ACN−TCNE system in solution and solid state. Participation of two distinct radical ion pairs was confirmed depending on the mode of excitation: the CIP from the CT excitation of the CT complex and the SSIP in the direct excitation of ACN.

Direct irradiation of ACN in solution in the presence of TCNE produces the SSIP, which gives *cisoid*-**1** and *transoid*-**1** as the major products together with **2**−**4** as minor products.

At low [ACN], the Φ_R and the *cisoid*/*transoid* ratio for the dimerization of ACN steeply increased and leveled off with increase of [TCNE]. Under this condition, the T_1 state of ACN undergoes ET to TCNE to generate the triplet SSIP competing with addition to the ground state of ACN. The dimerization exclusively proceeds via the triplet SSIP at high [TCNE] corresponding to the plateau region of Φ_R and the *cisoid*/*transoid* ratio. The triplet SSIP dissociates to free radical ions, $ACN^{+\bullet}$ and $TCNE^{-\bullet}$, and the former reacts with the ground-state ACN to give a dimeric radical cation, *cisoid*-$\mathbf{1}^{+\bullet}$ and *transoid*-$\mathbf{1}^{+\bullet}$, followed by charge recombination with $TCNE^{-\bullet}$ to give *cisoid*-**1** and *transoid*-**1**, respectively. The total efficiency (x_T) from the T_1 state to afford **1** can be obtained as 0.023 and 0.11 in DCE and AN, respectively.

At high [ACN], increase of [TCNE] reduced the Φ_R to an almost constant value but increased the *cisoid*/*transoid* ratio up to a nearly plateau value. In this condition the S_1 state of ACN undergoes ET to TCNE to afford the singlet SSIP competing with deactivation to the ground state. The fraction of survival (x_S) from the singlet SSIP to **1** is estimated to be 0.017 and 0.015 in DCE and AN, respectively.

A cycloadduct (**2**) results from geminate reaction in the SSIP as well as from coupling of free $ACN^{+\bullet}$ and $TCNE^{-\bullet}$. Formation of **3** and **4** only at high [ACN] is attributed to a preferred interaction of an ACN molecule with a singlet SSIP.

On the other hand, use of FN in place of TCNE did not affect at all Φ_R and the *cisoid*/*transoid* ratio of **1**. Therefore, $ACN^{+\bullet}$ and $FN^{-\bullet}$ do not participate in the dimerization because of the slightly positive ΔG_{ET} value for ET in ACN−FN.

In contrast to direct excitation of ACN, selective excitation of the CT complex between ACN and TCNE in DCE and AN did not result in any reaction. Excitation of the CT complex results in formation of CIP which undergoes very rapid BET preceding dissociation to free radical ions through SSIP since the CIP lies only 1.34 V above the ground state.

It is noteworthy that CT excitation of the 1:1 crystalline CT complex between ACN and TCNE afforded **2** as the sole product in contrast to ineffective CT excitation in solution. This distinctive reactivity and selectivity for product distribution in the crystalline CT complex is attributed to proximity and rigid mobility of the alkenic C═C double bonds of ACN and TCNE in ACN·TCNE, which retards the deactivation and BET but enables the two alkenic parts to undergo cycloaddition. Formation of $ACN^{+\bullet}$ as an intermediate was also confirmed by formation of *cisoid*-**1** and *transoid*-**1** on CT excitation of the mixed powder of ACN and TCNE.

Experimental Section

General. Common analytical instruments (melting point, ^{1}H NMR, ^{13}C NMR, UV, EI-MS, GC) are the same as in our previous papers.[21] Flash column chromatography and thin-layer chromatography (TLC) were performed on silica gel as described elsewhere.[53] Microanalyses were carried out in the microanalytical laboratory of our school.

Materials and Solvents. Purification of ACN has been described elsewhere.[21] TCNE (Tokyo Kasei) was purified by recrystallization from 1,2-dichlorobenzene followed by sublimation to give colorless prisms with mp 200.5−202.0 °C in a sealed capillary (lit.[26] mp 200−202 °C), which was analytically pure. No trace of impurity was detected on ^{13}C NMR spectrum. FN (Tokyo Kasei) was recrystallized from methanol. Potassium ferrioxalate was synthesized according to the literature.[54] Spectral-grade DCE and AN (Dojin) as solvents for photolysis were used as supplied.

Apparatus for Photolysis. Apparatus kit for preparative-scale irradiation in solution has been described elsewhere.[21,53,55] As the light source, a high-pressure mercury lamp was employed with color-glass filters. For isolation of light of wavelength longer than 300 nm, a jacket made of Pyrex glass was employed in stead of a quartz one. For reaction in solid state, a Pyrex vessel, in which disk color-glass filters with samples and argon gas are sealed, was used in a thermostat.

Merry-go-round apparatus for analytical-scale irradiation is described elsewhere.[55] For irradiation with light of wavelength longer than 400 and 500 nm, additional color-glass filters, HOYA L-42 (corresponds to Corning 3389) and HOYA Y-50 (corresponds to Corning 3486), were used, respectively. Temperature of sample solutions was maintained at 20 ± 2 °C in a thermostat.

Irradiation of ACN in the Presence of TCNE or FN. As a typical run, irradiation of ACN in the presence of TCNE in DCE will be described. A solution of 259 mg (1.70 mmol) of ACN and a solution of 218 mg (1.70 mmol) of TCNE in 170 mL of DCE was mixed and purged with nitrogen for 30 min prior to the irradiation. This solution was irradiated with >300-nm light at ambient temperature for 12 h. Bubbling of nitrogen gas was continued during the irradiation. After

(53) Haga, N.; Takayanagi, H. *J. Org. Chem.* **1996**, *61*, 735−745.
(54) Kuhn, H. J.; Braslavsky, S. E.; Schmidt, R. *Pure. Appl. Chem.* **1989**, 61, 188−210.
(55) Haga, N.; Kuriyama, Y.; Takayanagi, H.; Ogura, H.; Tokumaru, K. *Photochem. Photobiol.* **1995**, *61*, 557−562.

evaporation of the solvent under reduced pressure, the residual solid (428 mg) was flash-chromatographed (silica gel, eluent: hexane), which gave 48.1 mg (18.6%) of ACN, 25.2 mg (9.7%) of *cisoid*-**1**, and 39.3 mg (15.2%) of *transoid*-**1**. Further elution (hexane/dichloromethane, 2:1 then 1:1) gave 32.2 mg (8.8%) of the **3**, 19.5 mg (5.3%) of **4**, and 14.2 mg (3.0%) of **2**. Irradiation in AN gave a similar result.

The five products decompose in this irradiation condition, which caused low yield for them. Light of wavelength longer than 400 nm was used in an analytical scale, and the product distribution was determined by ^{1}H NMR without isolation. The results are summarized in Table 2.

8a,*t*-6b,*c*-6c,*c*-8a,6b,6c,12b-Tetrahydro[*c*,*e*]diacenaphthylene-13,13,14,14-tetracarbonitrile (3): recrystallized from dichloromethane−hexane, colorless prisms, mp 263.0−269.0 °C (dec.) EI-MS: *m*/*e* 432 (M^+). ^{1}H NMR ($CDCl_3$): δ 7.82−7.95 (m, 5H), 7.77 (d, 1H, J = 8.2 Hz), 7.60−7.73 (m, 4H), 7.40 (dd, 1H, J = 8.2, 7.0 Hz), 7.28 (dd, 1H, J = 7.0, 1.3 Hz), 5.28 (dd, 1H, J = 6.2, 5.3 Hz), 4.69 (d, 1H, J = 6.2 Hz), 4.69 (dd, J = 10.8, 5.3 Hz), 4.28 (d, 1H, J = 10.8 Hz). ^{13}C NMR ($CDCl_3$): δ 138.56, 137.54, 137.17, 137.01, 136.70, 134.74, 131.73, 131.67, 128.62, 128.42, 128.32 × 2, 127.62, 126.36, 125.44, 122.73, 122.08, 120.42, 119.46, 111.87, 110.87, 109.31, 109.22, 52.14, 47.93, 47.34, 47.20, 44.46, 43.29. Anal. Calcd for $C_{30}H_{16}N_4$: C, 83.32; H, 3.73; N, 12.95. Found: C, 83.52; H, 3.78; N, 12.97.

8a,*t*-6b,*t*-6c,*c*-8a,6b,6c,12b-Tetrahydro[*c*,*e*]diacenaphthylene-13,13,14,14-tetracarbonitrile (4): recrystallized from dichloromethane, pale-brown prisms, mp 284.0−292.0 °C (dec.) EI-MS: *m*/*e* 432 (M^+). ^{1}H NMR ($CDCl_3$): δ 8.00 (d, 1H, J = 7.0 Hz), 7.91−7.96 (m, 2H), 7.80−7.90 (m, 4H), 7.63−7.79 (m, 5H), 4.71 (dd, J = 10.0, 6.6 Hz), 4.64 (d, J = 6.7 Hz), 4.50 (d, J = 10.5 Hz), 4.36 (dd, J = 10.5, 10.0 Hz). Anal. Calcd for $C_{30}H_{16}N_4$: C, 83.32; H, 3.73; N, 12.95. Found: C, 83.56; H, 3.75; N, 12.94.

6b,8a-Dihydrocyclobut[*a*]acenaphthylene-7,7,8,8-tetracarbonitrile (2): recrystallized from dichloromethane, colorless prisms, slightly colored at 194 °C and decomposed at 293.0 °C in a sealed tube (lit.[36] dec. at 186 °C). EI-MS: *m*/*e* 280 (M^+). ^{1}H NMR ($CDCl_3$): δ 7.96 (d, 2H, J = 8.4 Hz), 7.73 (t, 2H, J = 8.4 Hz), 7.65 (d, 2H, J = 8.4 Hz), 5.13 (s, 2H). Anal. Calcd for $C_{18}H_8N_4$: C, 77.13; H, 2.88; N, 19.99. Found: C, 77.03; H, 3.12; N, 19.89.

Irradiation of ACN in the presence of FN was done in a similar manner as described above.

6b,*t*-7,*t*-8,*c*-6b,8a-Dihydrocyclobut[*a*]acenaphthylene-7,8-dicarbonitrile (5): recrystallized from dichloromethane−hexane, colorless needles, mp 186−187 °C. EI-MS: *m*/*e* 230 (M^+). ^{1}H NMR ($CDCl_3$): δ 7.79 (d, 2H, J = 8.0 Hz), 7.58 (dd, 2H, J = 8.0, 7.1 Hz), 7.46 (d, 2H, J = 7.1 Hz), 4.70 (d, 2H, J = 4.0 Hz), 3.3.41 (dd, 2H, J = 4.0, 1.4 Hz). Anal. Calcd for $C_{16}H_{10}N_2$: C, 83.46; H, 4.38; N, 12.17. Found: C, 83.55; H, 4.52; N, 12.04.

6b,*t*-7,*c*-8,*t*-6b,8a-Dihydrocyclobut[*a*]acenaphthylene-7,8-dicarbonitrile (6): recrystallized from ethanol, colorless fine fibers, mp 314−319 °C (dec. in a sealed tube). EI-MS: *m*/*e* 230 (M^+). ^{1}H NMR ($CDCl_3$): δ 7.83 (d, 1H, J = 8.2 Hz), 7.78 (d, 1H, J = 8.2 Hz), 7.65 (dd, J = 8.0, 7.0 Hz), 7.52−7.57 (m, 2H), 7.40 (d, 1H, J = 7.0 Hz). Anal. Calcd for $C_{16}H_{10}N_2$: C, 83.46; H, 4.38; N, 12.17. Found: C, 83.70; H, 4.47; N, 12.06.

6b,*c*-7,*c*-8,*c*-6b,8a-Dihydrocyclobut[*a*]acenaphthylene-7,8-dicarbonitrile (7): recrystallized from acetone, colorless prisms, mp 228−230 °C. EI-MS: *m*/*e* 230 (M^+). ^{1}H NMR ($CDCl_3$): δ 7.83 (d, 2H, J = 8.2 Hz), 7.63 (dd, 2H, J = 8.2, 7.0 Hz), 7.46 (d, 2H, J = 7.0 Hz), 4.60 (d, 2H, J = 10.0 Hz), 4.23 (d, 2H, J = 10.0 Hz). Anal. Calcd for $C_{16}H_{10}N_2$: C, 83.46; H, 4.38; N, 12.17. Found: C, 83.72; H, 4.54; N, 12.26.

Quantum Yields for Photodimerization of ACN in the Presence of TCNE or FN on Direct Excitation of ACN. Monochromatic light for measurement of quantum yields of 435.8 and 546.1 nm light has been described elsewhere.[21] Detailed procedure for the quantum yields measurements is similar as in the case our previous report employing ferrioxalate actinometry.[21] Irradiation time was controlled to keep the conversion low.

Preparation of the Crystalline CT Complex of ACN and TCNE. An equimolar solution of ACN and TCNE in ethyl acetate, which was prepared independently, was mixed. The solution was allowed to stand in the dark at ambient temperature for several days to evaporate the solvent slowly. Tan-brown prisms obtained were collected by filtration and dried in vacuo. Other solvents except ethyl acetate gave worse results. ACN·TCNE: mp 103.0−105.0 °C. Anal. Calcd for $C_{18}H_8N_4$: C, 77.13; H, 2.88; N, 19.99. Found: C, 77.10; H, 3.05; N, 20.19.

Irradiation of the Crystalline CT Complex. The crystalline CT complex (40.0 mg) was placed between two disk glass filters (Y-50) with a diameter of 120 mm and was irradiated for 7.0 h under argon atmosphere. The temperature was maintained at 20.0 ± 1.0 °C in a thermostat by circulating purified water. The resulting mixture was isolated by flash-chromatography (eluent: hexane then hexane−dichloromethane, 1:1), which gave 15.2 mg (74.6%) of ACN and 8.2 mg (80.7%) of **2** based on ACN consumed. When ACN was excited directly in the crystalline CT complex, L-42 filter was used instead of Y-50 filter.

In the case of irradiation of the mixed powder, an equimolar mixture of ACN and TCNE was pulverized in a mortar made of agate to develop tan-brown colorization. This powder was placed on the color-glass filter and irradiated in a similar manner as described above. The quantum yield for the solid-state reaction was determined according to Ito et al.[56]

X-ray Crystallographic Analysis. A single crystal with dimensions of 0.3 × 0.3 × 0.2 mm (**3**), 0.2 × 0.2 × 0.2 mm (**7**), and 0.4 × 0.6 × 0.3 mm (ACN·TCNE) was used for the analysis. Crystals of **3** undergo gradual crumbling on standing, so the single crystal was coated with adhesion during the data collection. The cell dimension and diffraction intensities were measured on a Rigaku AFC5R diffractometer using graphite monochromatic Cu Ka radiation (λ = 1.541 78 Å) and 12 kW rotating anode generator at 23 °C. The data were collected using the $\omega - 2\theta$ scan technique in the range of 2θ < 140.1°, 140.1°, and 126.5, for **3**, **7**, and ACN·TCNE, respectively. Scans of (1.10 + 0.30 tan θ)° at a speed of 32.0° min^{-1}, (1.78 + 0.30 tan θ)° at a speed 8.0° min^{-1}, and (1.78 + 0.30 tan θ)° at a speed of 32.0° min^{-1} were made for **3**, **7**, and ACN·TCNE, respectively. Total reflections of 4716, 1244, and 2813 were collected for **3**, **7**, and ACN·TCNE for Lorentz and polarization factors but not for absorption. The structures were elucidated by a direct method using TEXSAN.[57] At the final stage, the non-hydrogen atoms were refined anisotropically by the full-matrix least-squares refinement. A difference Fourier synthesis was calculated, and the positions of all hydrogen atoms were found and refined isotropically. Details of the crystal data are summarized in Table 1.

Acknowledgment. This work was partly supported by a Grant-in Aid for Scientific Research (No. 08640696, N.H.) from the Ministry of Education, Science, and Culture, Japan, and Kitasato University Research Grant for Young Researchers.

Registry Numbers: ACN, 208-96-8; TCNE, 670-54-2; *cisoid*-**1**, 15065-28-8; *transoid*-**1**, 14620-98-5; **2**, 35427-85-1; FN, 764-42-1.

Supporting Information Available: Positional parameters, *B*(eq), bond distances, bond angles, and torsion or conformation angles for **3**, **7**, and ACN·TCNE (27 pages). This material is contained in libraries on microfiche, immediately follows this article in the microfilm version of the journal, and can be ordered from the ACS; see any current masthead page for ordering information.

JO9801824

(56) Ito, Y.; Matsuura, T.; Fukuyama, K. *Tetrahedron Lett.* **1988**, *29*, 3087−3090.

(57) TEXRAY Structure Analysis Package; Molecular Structure Corp., 1985.